

Joint Antenna Position and Beamforming Optimization with Self-Interference Mitigation in MA-ISAC system

Size Peng*, Cixiao Zhang*, Yin Xu, Xiaowu Ou, and Dazhi He

Cooperative Medianet Innovation Center (CMIC), Shanghai Jiao Tong University, Shanghai 200240, China

Email: {sjtu2019psz, cixiaozhang, xuyin, xiaowu_ou, hedazhi}@sjtu.edu.cn

Abstract—Beamforming design has been extensively investigated in integrated sensing and communication (ISAC) systems. The use of movable antennas has proven effective in enhancing the design of beamforming. Although some studies have explored joint optimization of transmit beamforming matrices and antenna positions in bistatic scenarios, there is a gap in the literature regarding monostatic full-duplex (FD) systems. To fill this gap, we propose an algorithm that jointly optimizes the beamforming and antenna positions at both the transmitter and the receiver in a monostatic FD system. In an FD system, suppressing self-interference is crucial. This interference can be significantly reduced by carefully designing transmit and receive beamforming matrices. To further enhance the suppression, we derive a formulation of self-interference characterized by antenna position vectors. This enables the strategic positioning of movable antennas to further mitigate interference. Our approach optimizes the weighted sum of communication capacity and mutual information by simultaneously optimizing beamforming and antenna positions for both transceivers. Specifically, we propose a coarse-to-fine grained search algorithm (CFGS) to find optimal antenna positions. Numerical results demonstrate that our proposed algorithm provides significant improvements for the MA system compared to conventional fixed-position antenna systems.

Index Terms—Integrated sensing and communication, beamforming, Movable antenna, monostatic full-duplex system, self-interference, joint transceiver optimization, Coarse-to-Fine grained searching (CFGS).

I. INTRODUCTION

An increasing demand for reliable sensing and efficient communication has sparked significant interest in Integrated Sensing and Communication (ISAC) technologies. ISAC aims to merge communication and sensing functions within a single system, utilizing the same frequency bands and hardware resources. This integration optimizes spectral resource utilization, reduces hardware costs, and simplifies system complexity, positioning ISAC as a highly promising and efficient approach for modern wireless networks. Recent studies [1]–[3] indicate that ISAC systems can achieve notable improvements in spectral efficiency compared to traditional systems that separate these functions. As wireless networks advance towards 6G and beyond, ISAC is expected to play a crucial

role in meeting the growing demands for higher data rates, lower latency, and improved connectivity.

Beamforming design is critical in both MIMO communication and sensing systems due to its precoding capabilities. However, traditional systems with fixed, equally spaced antennas cannot fully exploit the spatial degrees of freedom (DOF) offered by the antennas. To address this limitation, a movable antenna (MA) system, also known as a fluid antenna system, has been proposed. This system can adjust antenna spacing using flexible RF chains, capturing the spatial variations of wireless channels. This approach has proven effectiveness in enhancing MIMO performance by jointly optimizing the precoding matrix and the positions of the transmit antenna, as demonstrated in [4].

Although some existing studies have explored the use of movable antennas in ISAC scenario [5]–[7], they do not consider an full-duplex (FD) scenario under ISAC. This paper pioneers the investigation of the effectiveness of movable antennas in a monostatic FD setup, which is a common scenario in ISAC. In particular, self-interference cancellation (SIC) is a critical issue in FD operation. High performance can only be achieved with sufficient SIC. Unlike physical isolation methods, active suppression of SI can be achieved through Tx and Rx beamforming [8], [9]. Motivated by [9]–[11], we model the SI channel as a near-field channel and formulate the SI channel characterized by the positions of the transmit and receive antennas, allowing for more precise control and reduction of SI.

We consider several clutters as sensing interferences in this monostatic FD system. To characterize the trade-off between communication and sensing, we use a weighted sum of communication rate and sensing mutual information (MI). The beamforming matrix and antenna positions at Tx and Rx are optimized using the alternating optimization (AO) method. Specifically, we propose a Coarse-to-Fine grained searching (CFGS) algorithm to determine the optimal antenna positions. Our contributions are threefold:

- We model the SI channel using the antenna position vectors of the transmitter and receiver. This enables the strategic positioning of MA to mitigate interference.
- We propose a method to jointly optimize the transmit and receive beamforming matrices along with the Tx/Rx

*These authors contributed equally to this work.
The corresponding author is Yin Xu (e-mail: xuyin@sjtu.edu.cn).

antenna positions.

- Numerical results demonstrate the effectiveness of our algorithm in enhancing performance in a monostatic FD ISAC system.

II. SYSTEM MODEL

In this paper, we consider a monostatic FD base station (BS) with N_T linear Tx-MA and N_R linear Rx-MA surrounded by K users, C clutters a sensing target. The antenna positions in Tx and Rx can move flexibly within the region $[X_{min}, X_{max}]$ and $[Y_{min}, Y_{max}]$, respectively.

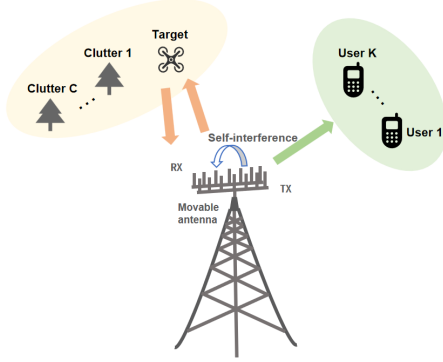


Fig. 1. System model of the monostatic MA-ISAC system.

A. Channel model

The antenna positions of Tx and Rx are denoted as $\mathbf{x} = [x_1, \dots, x_{N_T}]^T$ and $\mathbf{y} = [y_1, \dots, y_{N_R}]^T$. According to the far-field response model in [12], the transmit steering vector of Tx is

$$\mathbf{a}_{k,l}(\mathbf{x}) = [1 \quad e^{j\frac{2\pi}{\lambda}x_1 \cos(\theta_{k,l})} \quad \dots \quad e^{j\frac{2\pi}{\lambda}x_{N_T} \cos(\theta_{k,l})}]^T \in \mathbb{C}^{N_T}, \quad (1)$$

where $\theta_{k,l}$ denotes the angle of departure of l^{th} path of k^{th} user. Assume η_k is the free space fading factor and $\rho_{k,l}$ is the channel gain coefficient experienced by the l^{th} path of the k^{th} user. Therefore, the channel between the BS and the k^{th} user is

$$\mathbf{h}_k(\mathbf{x}) = \frac{\eta_k}{\sqrt{L_p}} \sum_{l=1}^{L_p} \rho_{k,l} \mathbf{a}_{k,l}(\mathbf{x}) \in \mathbb{C}^{N_T}. \quad (2)$$

Additionally, the receive steering vector for sensing is

$$\mathbf{b}(\mathbf{y}) = [1 \quad e^{j\frac{2\pi}{\lambda}y_1 \cos(\psi)} \quad \dots \quad e^{j\frac{2\pi}{\lambda}y_{N_R} \cos(\psi)}]^T \in \mathbb{C}^{N_R}, \quad (3)$$

Therefore, the channel model for sensing is

$$\mathbf{h}_s(\mathbf{x}, \mathbf{y}) = \frac{\eta_s}{\sqrt{L_p}} \sum_{l=1}^{L_p} \rho_s \mathbf{a}_s(\mathbf{x}) \mathbf{b}_s^H(\mathbf{y}) \in \mathbb{C}^{N_T \times N_R}. \quad (4)$$

Different from the far-field channel model, the self-interference channel should be modeled as near-field [9]–[11], [13]. We define $r(x_i, y_j)$ as the distance between the i^{th} transmit antenna and the j^{th} receive antenna. r_0 represents

the distance between X_{min} and Y_{min} . This distance can be expressed as

$$r(x_i, y_j) = \sqrt{r_0^2 + x_i^2 + y_j^2 + 2r_0 y_j \sin(\theta) - 2r_0 x_i \sin \theta - 2x_i y_j} \quad (5)$$

Thus, the self-interference channel model can be modeled as

$$\mathbf{H}_{SI}(\mathbf{x}, \mathbf{y}) = \left(\boldsymbol{\eta}_{SI} e^{-j\frac{2\pi}{\lambda} r_{x_i, y_j}} \right)_{N_T \times N_R}, \quad (6)$$

where

$$\boldsymbol{\eta}_{SI} = \frac{G_l}{4} \left[\left(\frac{\lambda}{2\pi r_{x_i, y_j}} \right)^2 - \left(\frac{\lambda}{2\pi r_{x_i, y_j}} \right)^4 + \left(\frac{\lambda}{2\pi r_{x_i, y_j}} \right)^6 \right]_{N_T \times N_R} \quad (7)$$

denotes the free space fading factor.

B. Signal model

Let $\mathbf{s} = [s_1, s_2, \dots, s_K]$ denotes the signals for K users, which is used for both communication and sensing. The transmit and receive beamforming matrix can be presented as

$$\mathbf{F} = [\mathbf{f}_1, \mathbf{f}_2, \dots, \mathbf{f}_K] \in \mathbb{C}^{N_T \times K}, \quad (8)$$

$$\mathbf{W} = [\mathbf{w}_1, \mathbf{w}_2, \dots, \mathbf{w}_{N_R}]^H \in \mathbb{C}^{N_R}. \quad (9)$$

Thus, the baseband received signal at k^{th} user is

$$r_k = \mathbf{h}_k^H(x) \mathbf{f}_k s_k + \mathbf{h}_k^H \sum_{j=1, j \neq k}^K \mathbf{f}_j s_j + n_k. \quad (10)$$

We can derive

$$\text{SINR}_k = \frac{|\mathbf{h}_k^H(x) \mathbf{f}_k|^2}{\sum_{j=1, j \neq k}^K |\mathbf{h}_k^H(x) \mathbf{f}_j|^2 + \sigma_k^2}. \quad (11)$$

Thus,

$$R_k = \log(1 + \text{SINR}_k). \quad (12)$$

Received signal at BS with receive beamforming is

$$r_s = \alpha_s \mathbf{w}^H \mathbf{b}_s(\mathbf{y}) \mathbf{a}_s^H(\mathbf{x}) \mathbf{F} \mathbf{s} + \sum_{c=1}^C \mathbf{w}^H (\alpha_c \mathbf{b}_c(\mathbf{y}) \mathbf{a}_c^H(\mathbf{x}) \mathbf{F} \mathbf{s}) + \mathbf{w}^H \mathbf{H}_{SI}(\mathbf{x}, \mathbf{y}) \mathbf{F} \mathbf{s} + \mathbf{w}^H \mathbf{n}_s. \quad (13)$$

Thus, we can get

$$\text{SCNR}_s = \frac{|\alpha_s \mathbf{w}^H \mathbf{b}_s(\mathbf{y}) \mathbf{a}_s^H(\mathbf{x}) \mathbf{F}|^2}{\sum_{c=1}^C |\alpha_c \mathbf{w}^H \mathbf{b}_c(\mathbf{y}) \mathbf{a}_c^H(\mathbf{x}) \mathbf{F}|^2 + |\mathbf{w}^H \mathbf{H}_{SI}(\mathbf{x}, \mathbf{y}) \mathbf{F}|^2 + \sigma_s^2}. \quad (14)$$

Following the approach in [5], [14], MI can be expressed as

$$R_s = \log(1 + \text{SINR}_s). \quad (15)$$

C. Problem formulation

To maximize the sum of communication rate and MI, weighted factors are introduced to establish the trade-off.

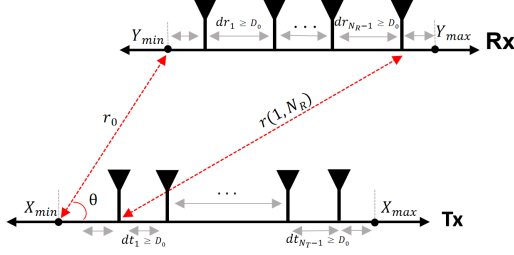


Fig. 2. Movable antenna model at Tx and Rx.

Furthermore, to prevent the coupling effect, it is necessary to maintain a minimum separation distance between each pair of antennas at the transmitter-receiver, i.e., $|x_i - x_j| \geq D_0, |y_j - y_i| \geq D_0, \forall i, \hat{i} \in \{1, \dots, N_T\}, \forall j, \hat{j} \in \{1, \dots, N_R\}, i \neq \hat{i}, j \neq \hat{j}$. As a result, the optimization problem is formulated as

$$(P1) \max_{\mathbf{F}, \mathbf{x}, \mathbf{y}, \mathbf{w}} \mathcal{G}(\mathbf{F}, \mathbf{x}, \mathbf{y}, \mathbf{w}) = \varpi_c \sum_{k=1}^K R_k + \varpi_s R_s, \quad (16a)$$

$$\text{s.t. } \text{Tr}(\mathbf{F}^H \mathbf{F}) \leq P_0, \quad (16b)$$

$$\mathbb{E}\{\mathbf{s}\mathbf{s}^H\} = \mathbf{I}, \quad (16c)$$

$$X_{min} \leq \mathbf{x} \leq X_{max}, Y_{min} \leq \mathbf{y} \leq Y_{max}, \quad (16d)$$

$$|x_i - x_j| \geq D_0, |y_j - y_i| \geq D_0, \forall i, \hat{i}, j, \hat{j}, i \neq \hat{i}, j \neq \hat{j}, \quad (16e)$$

where weighted factor ϖ_c and ϖ_s satisfy $\varpi_c + \varpi_s = 1$.

III. PROPOSED SOLUTION

It is challenging to solve the non-convex problem directly. Therefore, we introduce the auxiliary variables $\boldsymbol{\mu}$, $\boldsymbol{\xi}^c$, and $\boldsymbol{\xi}^s$ using a quadratic transformation to convert the equation (16a) into a convex form (25). Subsequently, we propose an AO algorithm, where the antenna positions, transmitter-receiver beamforming matrices, and auxiliary variables are updated alternately while keeping the others fixed.

A. Transmit and Receive Beamforming Optimization

We aim to optimize the transmit and receive beamforming matrix \mathbf{F} and \mathbf{w} with fixed \mathbf{x} , \mathbf{y} and auxiliary variables. Firstly, we formulate the subproblem for \mathbf{F}

$$(SP.1) \hat{\mathcal{G}}(\mathbf{F}|\mathbf{x}, \mathbf{y}, \mathbf{w}, \boldsymbol{\mu}, \boldsymbol{\xi}^c, \boldsymbol{\xi}^s) \text{ s.t. (16b)}. \quad (17)$$

Since $\hat{\mathcal{G}}$ is a convex function with respect to \mathbf{F} , we can employ the Lagrange dual method to obtain the closed-form expression of \mathbf{F} . The Lagrangian function is defined as $\mathcal{L}(\mathbf{F}, \lambda) = -\hat{\mathcal{G}}(\mathbf{F}|\mathbf{x}, \mathbf{y}, \mathbf{w}, \boldsymbol{\mu}, \boldsymbol{\xi}^c, \boldsymbol{\xi}^s) + \lambda (\text{Tr}(\mathbf{F}^H \mathbf{F}) - P_0)$.

The Lagrangian dual problem is then characterized by the following conditions:

$$\frac{\partial \mathcal{L}(\mathbf{F}, \lambda)}{\partial \mathbf{F}} = 0, \quad (18a)$$

$$\text{Tr}(\mathbf{F}^H \mathbf{F}) - P_0 \leq 0, \quad (18b)$$

$$\lambda \geq 0, \quad (18c)$$

$$\lambda (\text{Tr}(\mathbf{F}^H \mathbf{F}) - P_0) = 0, \quad (18d)$$

The closed form of \mathbf{F} can be obtained by solving (18a), which is

$$f_k(\lambda) = \left((\Lambda_k^T + \lambda \mathbf{I})^{-1} \right)^* \varphi_k^{(t)}, \quad (19)$$

where

$$\begin{aligned} \Lambda_k = & \varpi_s \|\boldsymbol{\xi}^s\|^2 \left\{ |\alpha_s|^2 (\mathbf{w}^H \mathbf{b}_s(\mathbf{y}) \mathbf{a}_s^H(\mathbf{x}))^H (\mathbf{w}^H \mathbf{b}_s(\mathbf{y}) \mathbf{a}_s^H(\mathbf{x})) \right. \\ & + \sum_{c=1}^C |\alpha_c|^2 (\mathbf{w}^H \mathbf{b}_c(\mathbf{y}) \mathbf{a}_c^H(\mathbf{x}))^H (\mathbf{w}^H \mathbf{b}_c(\mathbf{y}) \mathbf{a}_c^H(\mathbf{x})) \\ & \left. + (\mathbf{w}^H H_{SI}^H(x, y)) \left(\mathbf{w}^H H_{SI}^H(x, y) + \varpi_c h_k h_k^H \right) \right\} \quad (20) \end{aligned}$$

$$\begin{aligned} \phi_k = & \varpi_c \sqrt{1 + \mu_k} \boldsymbol{\xi}^{c(t)*} h_k(x^{(t)}) \\ & + \varpi_s \sqrt{1 + \mu_{K+1}} \alpha_s^* \boldsymbol{\xi}_k^{s(t)*} \mathbf{a}_s(x^{(t)}) b_s^H(y) \mathbf{w} \quad (21) \end{aligned}$$

Similarly, we can derive the closed form of \mathbf{w}

$$\mathbf{w} = \left\{ \{\Psi\}^{-1} \right\}^* \Upsilon, \quad (22)$$

where

$$\begin{aligned} \Psi = & \|\boldsymbol{\xi}^s\|^2 \left\{ \sum_c |\alpha_c|^2 (\mathbf{b}_c(\mathbf{y}) \mathbf{a}_c^H(\mathbf{x}) F) (\mathbf{b}_c(\mathbf{y}) \mathbf{a}_c^H(\mathbf{x}) F)^H \right. \\ & + |\alpha_s|^2 (\mathbf{b}_s(\mathbf{y}) \mathbf{a}_s^H(\mathbf{x}) F) (\mathbf{b}_s(\mathbf{y}) \mathbf{a}_s^H(\mathbf{x}) F)^H \\ & \left. + (H_{SI}^H(x, y) F) (H_{SI}^H(x, y) F)^H + \sigma_x^2 I \right\}, \quad (23) \end{aligned}$$

$$\Upsilon = \sqrt{1 + \mu_{K+1}} \alpha_s \mathbf{b}_s(\mathbf{y}) \mathbf{a}_s^H(\mathbf{x}) F \boldsymbol{\xi}^s. \quad (24)$$

To address λ in the complementary slackness condition, we draw inspiration from [5], [15] and employ a bisection method to select an appropriate dual variable.

$$\begin{aligned} \hat{\mathcal{G}}(\mathbf{F}, \mathbf{x}, \mathbf{y}, \mathbf{w}, \boldsymbol{\mu}, \boldsymbol{\xi}^c, \boldsymbol{\xi}^s) = & \varpi_c \sum_{k=1}^K \log(1 + \mu_k) + \varpi_s \log(1 + \mu_{K+1}) - \varpi_c \sum_{k=1}^K \mu_k - \varpi_s \mu_{K+1} \\ & + \varpi_c \sum_{k=1}^K \left[2\sqrt{1 + \mu_k} \text{Re}\{\boldsymbol{\xi}_k^c \mathbf{h}_k^H(\mathbf{x}) \mathbf{f}_k(\mathbf{x})\} - |\boldsymbol{\xi}_k^c|^2 \left(\sum_{j=1}^K |\mathbf{h}_k^H(\mathbf{x}) \mathbf{f}_j|^2 + \sigma_k^2 \right) \right] + \varpi_s \left[2\sqrt{1 + \mu_{K+1}} \text{Re}\{\alpha_s \mathbf{w}^H \mathbf{b}_s(\mathbf{y}) \mathbf{a}_s^H(\mathbf{x}) F \boldsymbol{\xi}^s\} \right. \\ & \left. - \|\boldsymbol{\xi}^s\|^2 \left(\sum_{c=1}^C \|\alpha_c \mathbf{w}^H \mathbf{b}_c(\mathbf{y}) \mathbf{a}_c^H(\mathbf{x}) F\|^2 + \|\mathbf{w}^H H_{SI}^H(x, y) F\|^2 + \|\alpha_s \mathbf{w}^H \mathbf{b}_s(\mathbf{y}) \mathbf{a}_s^H(\mathbf{x}) F\|^2 + \|\mathbf{w}\|^2 \sigma_s^2 \right) \right] \quad (25) \end{aligned}$$

B. Auxiliary Variables Optimization

With fixing other parameters, we can update the auxiliary variables ξ^c, ξ^s for quadratic transform parameters by solving the following subproblems

$$(SP.2)\hat{\mathcal{G}}(\xi^s|\mathbf{F}, \mathbf{x}, \mathbf{y}, \mathbf{w}, \mu, \xi^c), \quad (26)$$

$$(SP.3)\hat{\mathcal{G}}(\xi^c|\mathbf{F}, \mathbf{x}, \mathbf{y}, \mathbf{w}, \mu, \xi^s). \quad (27)$$

The subproblems are both concave, thus we can derive the closed-form formula as

$$\xi^s = \frac{\sqrt{1 + \mu_{K+1}} (\alpha_s \mathbf{w}^H \mathbf{b}_s(\mathbf{y}) \mathbf{a}_s^H(\mathbf{x}) F)^*}{A} \quad (28)$$

$$A = \sum_{c=1}^C \|\alpha_c \mathbf{w}^H \mathbf{b}_c(\mathbf{y}) \mathbf{a}_c^H(\mathbf{x}) F\|^2 + \|\mathbf{w}^H H_{SI}^H(x, y) F\|^2 + \|\alpha_s \mathbf{w}^H \mathbf{b}_s(\mathbf{y}) \mathbf{a}_s^H(\mathbf{x}) F\|^2 + \|\mathbf{w}\|^2 \sigma_s^2 \quad (29)$$

Similarly, we can derive the closed form of ξ^c :

$$\xi^c = \frac{\sqrt{1 + \mu_{K+1}} (\mathbf{f}_k^{(t)})^H \mathbf{h}_k(\mathbf{x}^{(t)})}{\sum_{j=1}^K \left| \mathbf{h}_k^H(\mathbf{x}^{(t)}) \mathbf{f}_j^{(t)} \right|^2 + \sigma_k^2} \quad (30)$$

Next should handle the subproblem of μ

$$(SP.4)\hat{\mathcal{G}}(\mu|\mathbf{F}, \mathbf{x}, \mathbf{y}, \mathbf{w}, \xi^s, \xi^c). \quad (31)$$

This can be easily solved by taking the derivative of μ into zero, which gives:

$$\mu_k = \frac{(R_k)^2 + R_k \sqrt{(R_k)^2 + 4}}{2}, k \in \{1, \dots, K+1\}, \quad (32)$$

where $R_k = \text{Re} \{ \xi_k^c \mathbf{h}_k^H(\mathbf{x}) f_k(\mathbf{x}) \}$, $k = \{1, \dots, K\}$ and $R_{K+1} = \text{Re} \{ \alpha_s \mathbf{w}^H \mathbf{b}_s(\mathbf{y}) \mathbf{a}_s^H(\mathbf{x}) F \xi_s^s \}$

Consequently, we can summarize the algorithm to update the above parameters in **Algorithm 1**.

C. Antenna Positions Optimization

With fixed beamformers, we can update the antenna positions for both \mathbf{x} and \mathbf{y} by solving subproblems:

$$(SP.5)\hat{\mathcal{G}}(\mathbf{x}|\mathbf{F}, \mathbf{y}^{(t)}, \mathbf{w}, \mu, \xi^c, \xi^s) \text{ s.t.}(16d), (16e). \quad (33)$$

$$(SP.6)\hat{\mathcal{G}}(\mathbf{y}|\mathbf{F}, \mathbf{x}^{(t)}, \mathbf{w}, \mu, \xi^c, \xi^s) \text{ s.t.}(16d), (16e). \quad (34)$$

This problem is difficult to solve directly because of its non-convexity. Thus, we propose a two-stage approach that combines coarse and fine granularity methods for updating antenna positions.

Initially, a coarse search is conducted across grid location sets O_x and O_y to identify appropriate initialization positions. These sets consist of points starting from $x = 0$ and $y = 0$ with intervals of λ within the movable range. During this coarse-grained search, N_T points are selected from all possible subsets of O_x , and the objective function is evaluated after the parameters in **Algorithm 1** converge for one iteration. After evaluating all possible combinations, the set yielding

Algorithm 1 Iterative optimization for precoding matrix and received beamforming.

Initialization: Choose the upper bound and lower bound of λ as λ_{max} and λ_{min} , tolerance ϵ , power limit P_0 , Randomly initial $\xi_s, \xi_c, \mu, \mathbf{w}$, set iteration index $i=1$.

```

1: repeat
2:   Update  $\mathbf{F}^{(i)}$  with the following bisection method
3:   repeat
4:     Compute  $\lambda = (\lambda_{max} + \lambda_{min})/2$ 
5:     Update precoding matrix  $\mathbf{F}^{(i)}$  as (19)
6:     Compute power  $P$  of precoding matrix  $\mathbf{F}^{(i)}$ 
7:     if  $P > P_0$  then
8:        $\lambda_{min} = \lambda$ 
9:     else
10:       $\lambda_{max} = \lambda$ 
11:    end if
12:   until  $|P - P_0| < \epsilon$ 
13:   Update  $\mathbf{w}^{(i)}$  as (22)
14:   Update  $\xi_c^{(i)}$  as (30)
15:   Update  $\xi_s^{(i)}$  as (28)
16:   Update  $\mu^{(i)}$  as (32)
17:   Update iteration index  $i = i + 1$ 
18: until the value of (25) converge
Output: optimal  $\mathbf{F}^*, \mathbf{w}^*$ 

```

the highest objective function value is selected as the initial x . A similar approach is used to select the initial y .

Subsequently, fine-grained adjustments on the best initial points are made using the gradient projection method [4], [5]. The antenna positions $x_n, n \in \{1, \dots, N_T\}$, $y_m, m \in \{1, \dots, N_R\}$ can be alternatively optimized as

$$x_n^{(i+1)} = x_n^{(i)} + \delta^t \nabla_{x_n} \hat{\mathcal{G}}(\mathbf{x}|\mathbf{F}, \mathbf{y}, \mathbf{w}, \mu, \xi^c, \xi^s), \quad (35)$$

$$y_m^{(i+1)} = y_m^{(i)} + \delta^t \nabla_{y_m} \hat{\mathcal{G}}(\mathbf{y}|\mathbf{F}, \mathbf{x}, \mathbf{w}, \mu, \xi^c, \xi^s), \quad (36)$$

where i denotes the iteration number for antenna inter-loop and δ^t denotes the step size of the gradient descent method. Next, we use projection to meet (16d), (16e). The update process for the receive antenna positions is analogous to that of transmitter. For simplicity, the explanation will focus solely on the transmit antenna positions. We rearrange the antenna indices, i.e. $\mathbf{X}_{\min} \leq \hat{x}_1 \leq \hat{x}_2 \leq \dots \leq \hat{x}_{N_T} \leq \mathbf{X}_{\max}$. The final step involves projecting onto the feasible region, which entails sorting the updated values of x after the last round of gradient descent in ascending order, reassigning antenna indices accordingly, and then adjusting the antenna spacing.

$$\hat{x}_1^{(t+1)} = \begin{cases} \mathbf{X}_{\min}, & \text{if } \hat{x}_1 < \mathbf{X}_{\min}, \\ \hat{x}_1, & \text{if } \mathbf{X}_{\min} \leq \hat{x}_1 \leq \mathbf{X}_{\max} - (N-1)D_0, \\ \mathbf{X}_{\max} - (N-1)D_0, & \text{if } \hat{x}_1 > \mathbf{X}_{\max} - (N-1)D_0, \end{cases} \quad (37)$$

⋮

$$\hat{x}_n^{(t+1)} = \begin{cases} \hat{x}_{n-1} + D_0, & \text{if } \hat{x}_n < \hat{x}_{n-1} + D_0, \\ \hat{x}_n, & \text{if } \hat{x}_{n-1} + D_0 \leq \hat{x}_n \leq \mathbf{X}_{\max} - (N-n)D_0, \\ \mathbf{X}_{\max} - (N-n)D_0, & \text{if } \hat{x}_n > \mathbf{X}_{\max} - (N-n)D_0, \end{cases} \quad (38)$$

$$\hat{x}_N^{(t+1)} = \begin{cases} \hat{x}_{N-1} + D_0, & \text{if } \hat{x}_N < \hat{x}_{N-1} + D_0, \\ \hat{x}_N, & \text{if } \hat{x}_{N-1} + D_0 \leq \hat{x}_N \leq \mathbf{X}_{\max}, \\ \mathbf{X}_{\max}, & \text{if } \hat{x}_N > \mathbf{X}_{\max}. \end{cases} \quad (39)$$

After projection, we can get the optimal antenna positions. The overall algorithm can be summarized in **Algorithm 2**.

Algorithm 2 Proposed CFGS algorithm for updating the antenna positions at Tx and Rx.

Initialization: Generate all the possible position alignments of transmit antenna as $\{\zeta_{x1}, \zeta_{x2}, \dots, \zeta_{xs_x}\}$ from \mathbf{O}_X . generate all the possible position alignments of receive antenna as $\{\zeta_{y1}, \zeta_{y2}, \dots, \zeta_{ys_y}\}$ from \mathbf{O}_Y , set iteration index $l = 1$.

- 1: **for** $i = 1, 2, \dots, s_x$ **do**
- 2: Let $\mathbf{x} = \zeta_{xi}$
- 3: Converge $\mathbf{F}^{(i)}$ and $\mathbf{w}^{(i)}$ with algorithm 1
- 4: Compute $R_{xi} = \mathcal{G}(\mathbf{F}^{(i)}, \mathbf{x}, \zeta_{y1}, \mathbf{w}^{(i)})$
- 5: **end for**
- 6: Let $\mathbf{x}^{(0)} = \zeta_{xk}, k = \arg \max R_x$
- 7: **for** $j = 1, 2, \dots, s_y$ **do**
- 8: Let $\mathbf{y} = \zeta_{yj}$
- 9: Converge $\mathbf{F}^{(j)}$ and $\mathbf{w}^{(j)}$ with algorithm 1
- 10: Compute $R_{yj} = \mathcal{G}(\mathbf{F}^{(j)}, \mathbf{x}^{(0)}, \mathbf{y}, \mathbf{w}^{(j)})$
- 11: **end for**
- 12: Let $\mathbf{y}^{(0)} = \zeta_{yk}, k = \arg \max R_y$
- 13: **repeat**
- 14: Converge $\mathbf{F}^{(l)}$ and $\mathbf{w}^{(l)}$ with algorithm 1
- 15: Converge $\mathbf{x}^{(l)}$ and $\mathbf{y}^{(l)}$ as (35) and (36)
- 16: Adjust $\mathbf{x}^{(l)}$ and $\mathbf{y}^{(l)}$ as (37)-(39)
- 17: Update iteration index $l = l + 1$
- 18: **until** the value of (25) converge

Output: optimal transmit antenna position \mathbf{x}^* , optimal receive antenna position \mathbf{y}^*

IV. SIMULATION RESULTS

Two algorithms, which use the same beamforming updating method proposed in **Algorithm 1** but differ in antenna configuration, are used for comparison, including fixed Position Antenna (FPA) and gradient descent with movable antenna (GD-MA). In the FPA method, the antenna spaces of the transmit and receive antennas are $\lambda/2$. In the GD-MA method, the transmit and receive antennas are initially randomly located in the movable range and directly optimized with the gradient descent method as shown from **Step 13** to **Step 17** in **Algorithm 2**.

A Rayleigh channel with $L_p = 13$ paths is chosen with user number $K = 4$, clutter number $C = 3$. Users, sensing target and clutters are located randomly around the station.

The complex coefficients and the complex channel gain follow the standard complex Gaussian distribution, i.e. $\alpha_c, \alpha_s, \rho_s \sim \mathcal{CN}(0, 1)$. The free space fading factors for far-field are all set as $\eta = \left[\frac{\sqrt{G_t \lambda}}{4\pi d}\right]^2$. The movable range of transmit antenna is 1.5 metre which is 12 times wavelength and for receive antenna is 1 metre which is 8 times wavelength. \mathbf{O}_X and \mathbf{O}_Y are sets of points on movable range of transmit and receive antennas spaced by 1λ . Parameters of the simulation system are shown as **Table I** unless otherwise specified.

TABLE I
PARAMETERS OF THE MONO-STATI MA-ISAC SYSTEM

Parameter	Notation	Value
User and clutter angle	θ_u, θ_c	$[0, \pi]$
Number of transmit antenna	N_T	8
Number of receive antenna	N_R	4
Carrier wavelength	λ	0.01 m
Distance between user and BS	$d_{u,b}$	[50m,80m]
Distance between target and BS	$d_{t,b}$	[10m,20m]
Distance between Rx and Tx antenna gain	$d_{Tx,Rx}, G_l$	1.25 m, 1
Receive noise power	σ_r^2	-60 dBm
Transmit power	P	30dBm
Communication weighting factor	ϖ_c	0.5
Sensing weighting factor	ϖ_s	0.5

Fig.(3) shows the objective function with different transmit power and different number of antennas. The transmit power varies from 10 dBm to 40 dBm, and three sets of antenna numbers are used for simulation, which is 8, 10, 8 for transmit antennas and 4, 4, 6 for receive antennas. The result shows that the objective function grows with increasing transmit power and also with increasing number of transmit or receive antennas. When transmit power $P = 30$ dBm, 8 transmit antennas and 4 receive antennas are used. The objective function increases by 14.01% with GD-MA compared to FPA, and a 35.69% increment when CFGS-MA is used compared to FPA. Furthermore, for all three sets of antennas number in the simulation, CFGS-MA shows a better result than GD-MA and FPA.

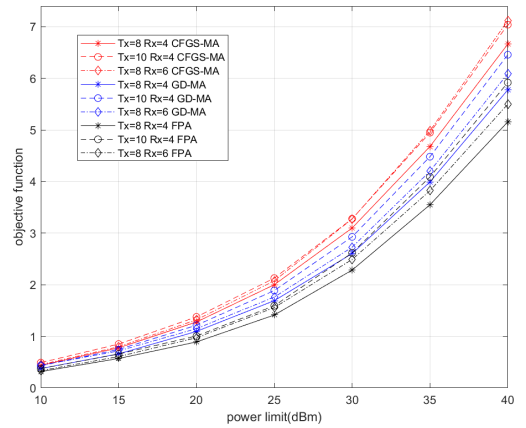


Fig. 3. Objective function with different transmit power.

Fig.(4) shows the result with different movable range of

transmit and receive antennas. The movable range of transmit antenna varies from 8 to 14 λ , and receive antenna range for 6, 8 and 10 λ . As shown in the result, when GD-MA is used, the result just have a slightly improve since GD-MA can only get a local optimum around the initial position, which can not make full use of the larger movable range. As for CFGS-MA, there is a 13.67% increment of objective function as the movable range of transmit antennas grows from 8 to 14 λ while the movable range of receive antennas is 8 λ . And a 2.81% increment as the movable range of receive antennas varies from 6 to 10 λ while transmit antennas movable range is 12 λ . The above result shows that CFGS-MA could make good use of movable range.

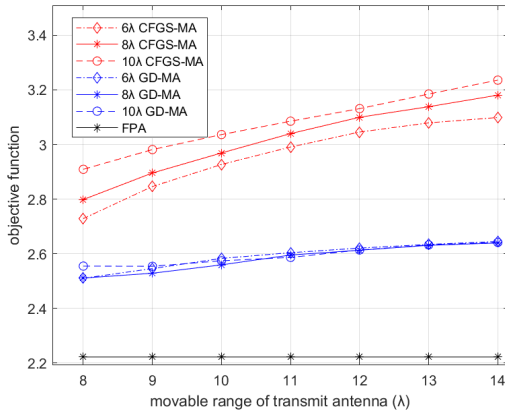


Fig. 4. Objective function with different antenna movable range.

Fig.(5) shows the trade-off between communication and sensing by varying ϖ_c from 0.1 to 0.9. Additionally, different $d_{Tx,Rx}$ which effects in self interference are compared. The result shows that as the $d_{Tx,Rx}$ become larger, which leading to a lighter self interference, there is a larger rate in most situation. And CFGS-MA could still outperform GD-MA even with greater interference.

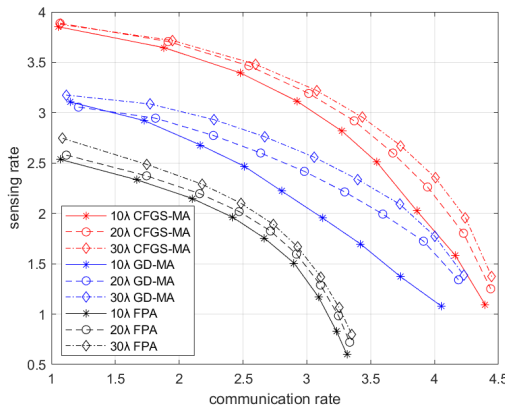


Fig. 5. Trade-off between communication and sensing with different self-interference.

V. CONCLUSION

This paper focuses on maximizing the communication rate and mutual information in a monostatic MA-ISAC system.

We derive the self-interference channel formula which allows the system to effectively suppress interference. To address the non-convexity of the objective function, we use the FP method to transform the formula. The problem is divided into six subproblems using the AO method. In particular, for the optimization of antenna positions, we compare the proposed CFGS method with the GD-MA and FPA configurations. Numerical results demonstrate that CFGS offers significant advantages under various conditions.

REFERENCES

- [1] Zhenyao He, Wei Xu, Hong Shen, Derrick Wing Kwan Ng, Yonina C. Eldar, and Xiaohu You, "Full-duplex communication for isac: Joint beamforming and power optimization," *IEEE Journal on Selected Areas in Communications*, vol. 41, no. 9, pp. 2920–2936, 2023.
- [2] Fan Liu, Christos Masouros, Athina P. Petropulu, Hugh Griffiths, and Lajos Hanzo, "Joint radar and communication design: Applications, state-of-the-art, and the road ahead," *IEEE Transactions on Communications*, vol. 68, no. 6, pp. 3834–3862, 2020.
- [3] Fan Liu, Yuanhao Cui, Christos Masouros, Jie Xu, Tony Xiao Han, Yonina C. Eldar, and Stefano Buzzi, "Integrated sensing and communications: Toward dual-functional wireless networks for 6g and beyond," *IEEE Journal on Selected Areas in Communications*, vol. 40, no. 6, pp. 1728–1767, 2022.
- [4] Guojie Hu, Qingqing Wu, Kui Xu, Jiangbo Si, and Naofal Al-Dhahir, "Secure wireless communication via movable-antenna array," *IEEE Signal Processing Letters*, vol. 31, pp. 516–520, 2024.
- [5] Wanting Lyu, Songjie Yang, Yue Xiu, Zhongpei Zhang, Chadi Assi, and Chau Yuen, "Flexible beamforming for movable antenna-enabled integrated sensing and communication," *arXiv preprint arXiv:2405.10507*, 2024.
- [6] Chao Wang, Guo Li, Haibin Zhang, Kai-Kit Wong, Zan Li, Derrick Wing Kwan Ng, and Chan-Byoung Chae, "Fluid antenna system liberating multiuser mimo for isac via deep reinforcement learning," *IEEE Transactions on Wireless Communications*, pp. 1–1, 2024.
- [7] Tian Hao, Changxin Shi, Yinghong Guo, Bin Xia, and Feng Yang, "Fluid-antenna enhanced integrated sensing and communication: Joint antenna positioning and beamforming design," *arXiv preprint arXiv:2407.05297*, 2024.
- [8] Kenneth E. Kolodziej, Bradley T. Perry, and Jeffrey S. Herd, "In-band full-duplex technology: Techniques and systems survey," *IEEE Transactions on Microwave Theory and Techniques*, vol. 67, no. 7, pp. 3025–3041, 2019.
- [9] Chengzhe Shi, Wensheng Pan, Ying Shen, and Shihai Shao, "Robust transmit beamforming for self-interference cancellation in star phased array systems," *IEEE Signal Processing Letters*, vol. 29, pp. 2622–2626, 2022.
- [10] Wei Zhang, Ziyu Wen, Cheng Du, Yi Jiang, and Bin Zhou, "Ris-assisted self-interference mitigation for in-band full-duplex transceivers," *IEEE Transactions on Communications*, vol. 71, no. 9, pp. 5444–5454, 2023.
- [11] Yu Lu and Linglong Dai, "Mixed los/nlos near-field channel estimation for extremely large-scale mimo systems," in *ICC 2023 - IEEE International Conference on Communications*, 2023, pp. 1506–1511.
- [12] Lipeng Zhu, Wenyan Ma, and Rui Zhang, "Modeling and performance analysis for movable antenna enabled wireless communications," *IEEE Transactions on Wireless Communications*, vol. 23, no. 6, pp. 6234–6250, 2024.
- [13] Hans Gregory Schantz, "Near field propagation law & a novel fundamental limit to antenna gain versus size," in *2005 IEEE Antennas and Propagation Society International Symposium*. IEEE, 2005, vol. 3, pp. 237–240.
- [14] Zhitong Ni, J. Andrew Zhang, Kai Yang, Xiaojing Huang, and Theodoros A. Tsiftsis, "Multi-metric waveform optimization for multiple-input single-output joint communication and radar sensing," *IEEE Transactions on Communications*, vol. 70, no. 2, pp. 1276–1289, 2022.
- [15] Cunhua Pan, Hong Ren, Kezhi Wang, Maged Elkashlan, Arumugam Nallanathan, Jiangzhou Wang, and Lajos Hanzo, "Intelligent reflecting surface aided mimo broadcasting for simultaneous wireless information and power transfer," *IEEE Journal on Selected Areas in Communications*, vol. 38, no. 8, pp. 1719–1734, 2020.